

New Journal of Physics

The open access journal at the forefront of physics

Deutsche Physikalische Gesellschaft 

IOP Institute of Physics

Published in partnership
with: Deutsche Physikalische
Gesellschaft and the Institute
of Physics



PAPER

OPEN ACCESS

RECEIVED
2 December 2015

REVISED
19 December 2016

ACCEPTED FOR PUBLICATION
23 December 2016

PUBLISHED
6 January 2017

Martin Rohden¹, Dirk Witthaut^{2,3,4}, Marc Timme⁴ and Hildegard Meyer-Ortmanns¹

¹ Jacobs University Bremen, Physics and Earth Sciences, D-28759 Bremen, Germany

² Forschungszentrum Jülich, Institute for Energy and Climate Research -Systems Analysis and Technology Evaluation (IEK-STE), D-52428 Jülich, Germany

³ Institute for Theoretical Physics, University of Cologne, D-50937 Köln, Germany

⁴ Network Dynamics, Max Planck Institute for Dynamics and Self-Organization (MPIDS), D-37077 Göttingen, Germany

E-mail: m.rohden@jacobs-university.de

Keywords: complex networks, power grids, rerouting, critical links, synchronization

Original content from this work may be used under the terms of the Creative Commons Attribution 3.0 licence.

Any further distribution of this work must maintain attribution to the author(s) and the title of the work, journal citation and DOI.



Abstract

Modern societies crucially depend on the robust supply with electric energy so that blackouts of power grids can have far reaching consequences. Typically, large scale blackouts take place after a cascade of failures: the failure of a single infrastructure component, such as a critical transmission line, results in several subsequent failures that spread across large parts of the network. Improving the robustness of a network to prevent such secondary failures is thus key for assuring a reliable power supply. In this article we analyze the nonlocal rerouting of power flows after transmission line failures for a simplified AC power grid model and compare different strategies to improve network robustness. We identify critical links in the grid and compute alternative pathways to quantify the grid's redundant capacity and to find bottlenecks along the pathways. Different strategies are developed and tested to increase transmission capacities to restore stability with respect to transmission line failures. We show that local and nonlocal strategies typically perform alike: one can equally well cure critical links by providing backup capacities locally or by extending the capacities of bottleneck links at remote locations.

1. Introduction

We are currently witnessing a rapid transition in power generation from conventional to renewable power sources. Typically, renewable power sources are strongly fluctuating, have a lower power output than conventional ones, and their potential geographical locations are restricted to places with sufficient solar or wind power [1, 2]. This development is challenging the operation and stability of electric power grids: power has to be transmitted over long distances [3], fluctuations must be balanced by storage or backup power plants [4–6], and many decentralized units must be controlled [7–9].

In general power grids work reliably, and power outages on a large scale are rare events [10–12]. However, just in the last decade major outages were recorded in India (2012), Bangladesh (2014), Pakistan (2015), Indonesia (2005), Brazil (2009), Turkey (2015) and Germany (2006). A detailed analysis of the latter outage can be found in [13]. Each of these outages affected millions of people with potentially destructive impact [14, 15]. It is commonly expected that the loads will increase strongly in future grids [3], so that these outages can become more likely. So it is urgent to trace back what causes such outages and to minimize the risk for these events to happen in the future. It may come as a surprise that large power outages in the past often were triggered by the outage of a single infrastructure component, such as a transmission line [11]. In such an event, after one transmission line failed, a second line became overloaded and initiated a whole cascade of further failures [16–22].

To exclude such outages induced by single component failures, the so-called ($N - 1$) rule is currently implemented in modern power grid operations. The ($N - 1$)-rule states that at every instant of time, the power grid has still to be fully functional even if any given single component, e.g., a transmission line, fails [23]. However, this criterion may be violated in times of high loads, as for example in Germany (2006). The

intentional shutdown of a single transmission line in Northern Germany brought the entire grid to the edge of a breakdown. A coupling of the busbars at a nearby transformer station then finally triggered the blackout, in which the European grid fragmented into three mutually asynchronous areas [13]. Additionally, an inclusion of new power sources into the grid is ongoing, and the need for additional transmission lines continues. Therefore it becomes more and more challenging to maintain the implementation of the ($N - 1$)-rule.

In this article we study how general supply networks can be cured from critical line failures by extending the transmission capacities. We use an AC power flow model based on the swing equation [24] to model the dynamics of the supply networks, so that the results are in principle also applicable for power grids. In particular, we analyze how much additional capacity is needed and where it can be inserted. We approach these questions in terms of a graph-theoretic max-flow problem to derive rigorous results and provide an insight into the robustness of complex supply networks. We quantify the redundancy of a grid with respect to line failures and identify the bottlenecks which limit the redundancy. The capacity needed to restore $N - 1$ -security can then be bounded from below by the lack of redundancy with respect to the flow prior to the link failure. This approach also shows where grid extensions should be placed. Typically, it plays a minor role whether capacity is increased locally or non-locally at the position of grid bottlenecks.

2. An oscillator model for power grid dynamics

In this article we focus on the stability of AC power grids with respect to transmission line outages. Consider a transmission line connecting two nodes j and ℓ of the grid with impedance $Z_{j\ell} = R_{j\ell} + iX_{j\ell}$, i being the imaginary unit. In high-voltage transmission grids, ohmic losses are typically small such that we can neglect the resistance R . The real power flow along this line from node j to node ℓ is then given by

$$F_{j\ell} = \operatorname{Re}(U_j I_{j\ell}^*), \quad (1)$$

where $I_{j\ell} = (U_j - U_\ell)/Z_{j\ell}$ is the electric current and U_j is the complex voltage at node j . Evaluating this expression, one finds

$$F_{j\ell} = \frac{|U_j U_\ell|}{X_{j\ell}} \sin(\theta_j - \theta_\ell), \quad (2)$$

where θ_j is the voltage phase angle. In the steady operation of a grid, the real power at each node must be balanced, i.e., the injected power P_j^{in} must equal the power transmitted to the grid for all nodes $j = 1, \dots, N$. In terms of the nodal voltage phase angles this condition reads

$$P_j^{\text{in}} = \sum_{\ell \in \mathcal{N}(j)} F_{j\ell} = \sum_{\ell \in \mathcal{N}(j)} \frac{|U_j U_\ell|}{X_{j\ell}} \sin(\theta_j - \theta_\ell) \quad \forall j = 1, \dots, N, \quad (3)$$

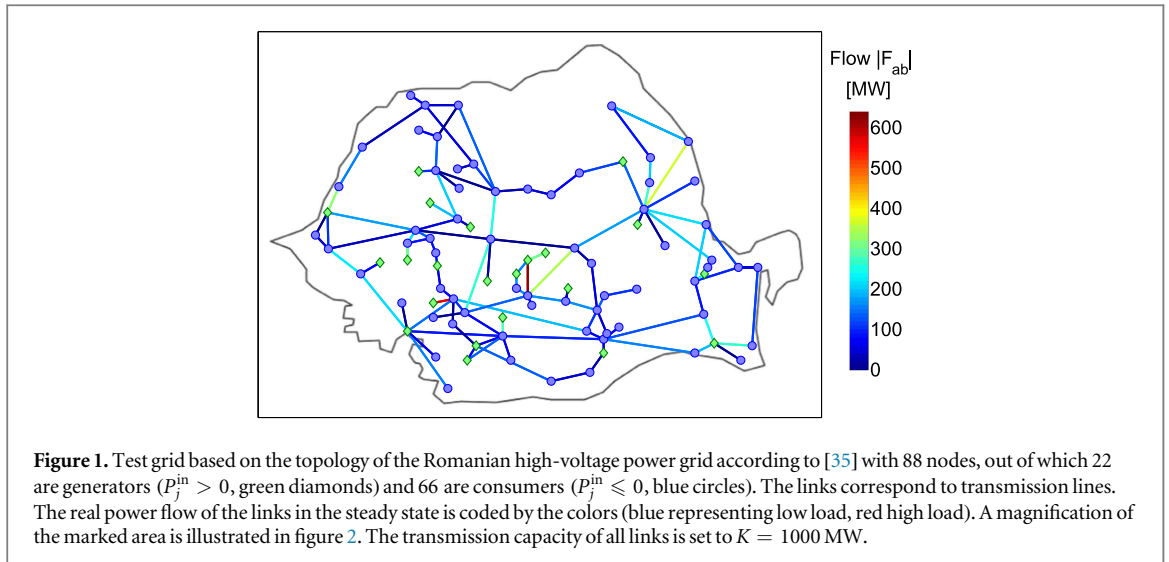
where $\mathcal{N}(j)$ denotes the immediate neighborhood of node j , i.e., the set of nodes connected to j . The injected power is the sum of the mechanical power and the load, $P_j^{\text{in}} = P_j^{\text{mech}} - P_j^{\text{load}}$. For generator nodes the injected power is positive with $P_j^{\text{mech}} > 0$ and $P_j^{\text{load}} = 0$, while for load nodes the injected power is negative with $P_j^{\text{mech}} = 0$ and $P_j^{\text{load}} > 0$. In this article we analyze whether this equation has a stable solution after the outage of a single transmission line and how stability can be recovered by local or non-local grid extensions. We concentrate on the real power flow in the grid, leaving aside problems of voltage stability or reactive power compensation. We thus assume that the voltages are given by their nominal values and define the transmission capacity of a line (j, ℓ) as $K_{j\ell} = |U_j U_\ell|/X_{j\ell}$ with $K_{j\ell} = 0$ if no line exists.

To assess the dynamical stability we further need a model for the dynamics of the single nodes. We concentrate on the rotor angle or frequency stability of the machines connected to the grid. Generators are modeled as rotating synchronous machines, whose voltage phase angle equals the mechanical rotor angle. Typically the rotor angle θ_j is given in a reference frame rotating at the nominal frequency $\omega_0 = 2\pi \times 50$ Hz or $\omega_0 = 2\pi \times 60$ Hz, respectively. The dynamics is then given by the swing equation [24]

$$\begin{aligned} M_j \frac{d^2\theta_j}{dt^2} + D_j \frac{d\theta_j}{dt} &= \frac{1}{\omega_0} (P_j^{\text{in}} - P_j^{\text{el}}) \\ &= \frac{1}{\omega_0} \left(P_j^{\text{in}} - \sum_{\ell} K_{j\ell} \sin(\theta_j - \theta_\ell) \right), \end{aligned} \quad (4)$$

where M_j is the machine's moment of inertia and D_j is a damping coefficient. The right hand side is the mechanical torque τ_j acting on the machine, which is related to the total power via $\omega_0 \cdot \tau_j$, ω_0 being the base frequency of the grid.

Different models have been used to describe the dynamics of load nodes and a comparison of models for synchronous machine operation can be found in [25–28]. In the classical model of electric power engineering



one assumes that loads are ohmic, which can be eliminated from the dynamics [24, 29]. Bergen and Hill introduced a model on the basis of the load-frequency characteristics of a load node, leading to an equation of motion of the form (4), however with inertia $M_j = 0$ [30, 31]. The loads are thus given by first order oscillators, while the generators are given by second order oscillators. Other models consider synchronous motors as models of the load, such that all nodes are equally modeled as second order oscillators [7, 32–34]. The dynamics of the load nodes is then exactly given by equation (4) with $P_j^{\text{in}} < 0$. In both cases the steady state of the grid is given by the algebraic equation

$$0 = P_j^{\text{in}} - \sum_{\ell} K_{j\ell} \sin(\theta_j - \theta_{\ell}), \quad (5)$$

which obviously coincides with the condition of real power balance for each node (3).

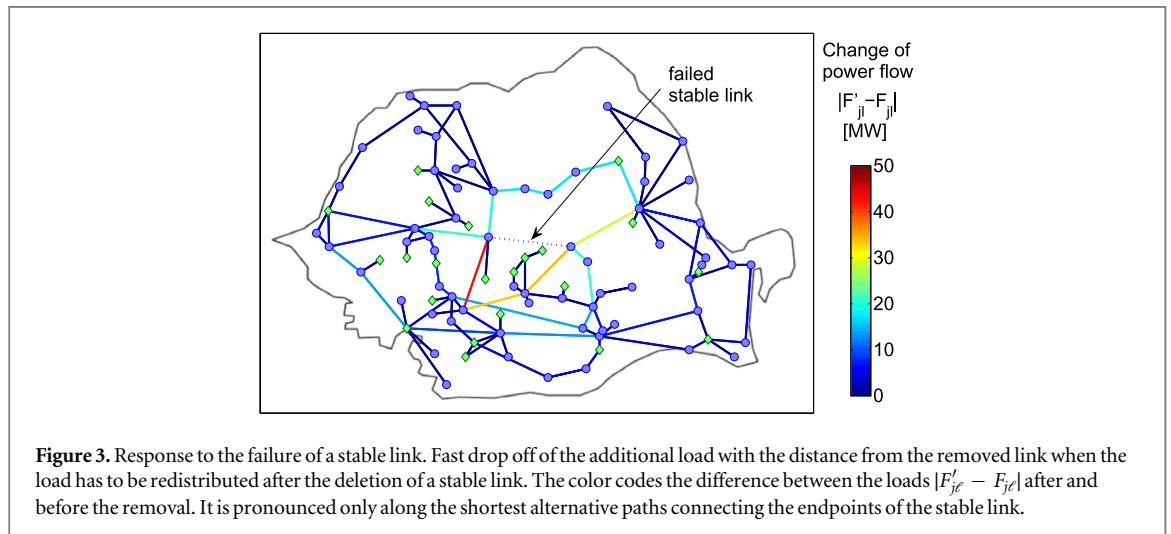
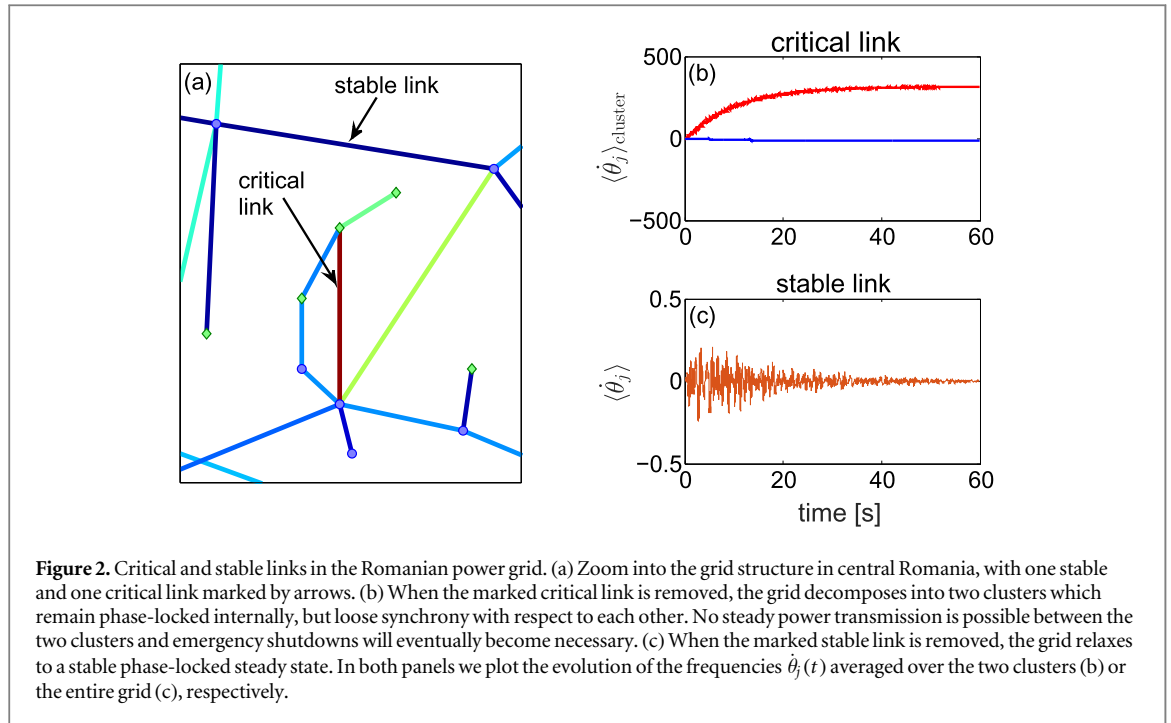
For the sake of simplicity, we choose to model all nodes as second order oscillators with equal values of the inertia $\omega_0 M_j \equiv 10^7$ kg m² s⁻¹ and the damping $\omega_0 D_j \equiv 10^6$ kg m² s⁻² and also assume that all transmission lines have the same transmission capacity K . The reason for this simplification is that we primarily focus on the strategies, in which the actual load models only enter in the identification of bottlenecks to be discussed below. Otherwise the strategies apply to different and also more realistic versions of the load models. We consider hypothetical power grids, which are heavily loaded and thus not $(N - 1)$ -secure in the first place. Such situations are rare nowadays, but are expected to become much more frequent in future highly renewable power grids (see, e.g., [3]).

3. Critical links and flow rerouting

A failure of a single transmission line can have different types of impact on the operation of the power grid as illustrated in figure 2. It may cause only weak transient disturbances such that the network relaxes back to a stable steady state, or it may destabilize the synchronous action of the machines and, in the extreme case, induce a cascade of failures that ends up in a large-scale power outage. We call links, whose failure leads to a desynchronization of the grid, ‘critical links’. All other links are referred to as stable. An example is demonstrated in figure 2, where a stable and a critical link are marked in panel (a). The response of the frequency to a failure of the marked critical link is illustrated in panel (b) and to the marked stable link in panel (c).

So suppose that the load in the grid is so large that some links are critical. We want to expand the grid to restore $N - 1$ -stability by building new links or by increasing the capacity of existing links. The central question addressed in this article is how much additional capacity is needed and where it can be inserted. One obvious strategy (called strategy A in the following) is to just duplicate every critical link to provide a backup. This strategy trivially restores $N - 1$ -stability but is rather costly in the sense that much additional capacity has to be added. The numerical examples studied in this paper (see figures 4–6) show that generally much less capacity is actually required. But how much additional capacity do we really need and where can we extend the grid?

To answer these questions we analyze the flow rerouting problem in more detail. So denote the flows before the outage by a superscript (0). We consider the failure of a link (a, b) assuming w.l.o.g. $F_{ab}^{(0)} \geq 0$, i.e., power flows from a to b before the failure. A necessary condition for stability after the failure of link (a, b) is that a stable fixed point still exists. We now derive a necessary conditions (10) for the existence of such a fixed point. If this condition is violated, then link (a, b) must be critical. Furthermore, we discuss how the condition can be restored



by grid extensions, which guides us in the formulation of algorithms for curing all critical links as detailed in section 4.

We denote the flows in the fixed point after the failure by $F_{j\ell}^{(0)} + \Delta F_{j\ell}$. The flows changes must satisfy

$$\sum_{\ell} \Delta F_{j\ell} = \begin{cases} +F_{ab}^{(0)} & j = a \\ -F_{ab}^{(0)} & \text{for } j = b \\ 0 & j \neq a, b \end{cases}, \quad (6)$$

i.e., we have to transmit the power $F_{ab}^{(0)}$ from a to b via an alternative route. Furthermore, the flow is limited by the transmission capacities

$$\begin{aligned} -K_{j\ell} &\leq F_{j\ell}^{(0)} + \Delta F_{j\ell} \leq K_{j\ell} \\ \Leftrightarrow -K_{j\ell} - F_{j\ell}^{(0)} &\leq \Delta F_{j\ell} \leq +K_{j\ell} - F_{j\ell}^{(0)} \end{aligned} \quad (7)$$

for all links (j, ℓ) . Whether such a flow can exist is a standard problem in graph theory. So define the weighted directed graph \tilde{G} , whose vertices are the oscillators and edges are the transmission lines. We have to consider a directed graph, because the bounds for the flow change (7) are asymmetric. Hence we define the edge weights in the graph \tilde{G} as

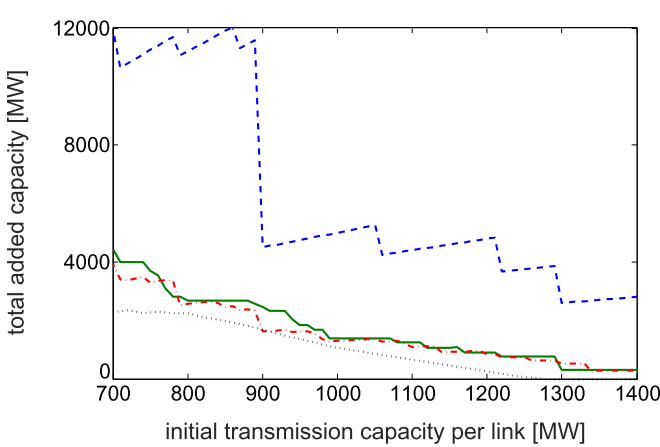


Figure 4. How much additional capacity is required to cure all critical links? We compare the three strategies defined in section 4: A: duplicating the critical line (blue dashed) B: adding a backup line of minimum capacity locally (red dash-dotted) C: adding capacity at bottlenecks nonlocally (solid green). The black dotted line shows the approximate lower bound (17). Results are shown for the test grid based on the topology of the Romanian power grid shown in figure 1.

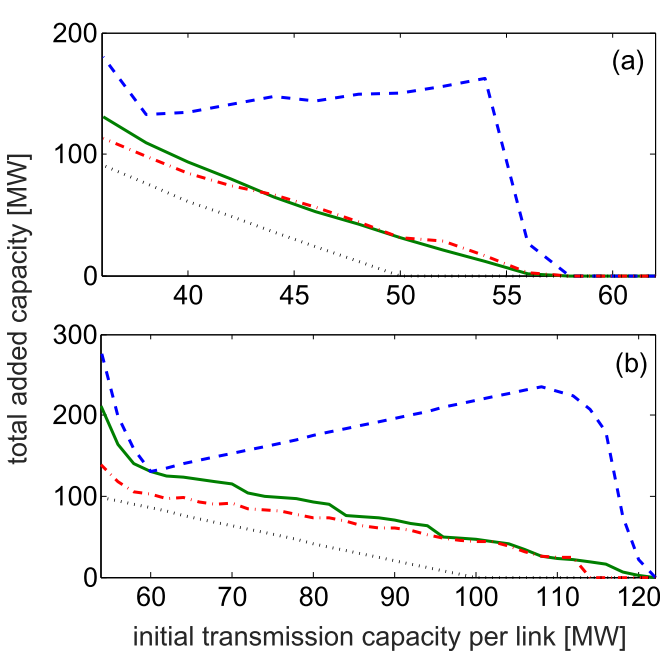


Figure 5. Comparison of strategies as in figure 4, but for random networks with an average degree of six (a) and four (b). We compare the three strategies defined in section 4: A: duplicating the critical line (blue dashed) B: adding a backup line of minimum capacity locally (red dash-dotted) C: adding capacity at bottlenecks nonlocally (solid green). The black dotted line shows the approximate lower bound (17).

$$\tilde{K}_{j \rightarrow \ell} = K_{j\ell} - F_{j\ell}^{(0)}. \quad (8)$$

The line (a, b) cannot carry any flow after the damage so we set

$$\tilde{K}_{a \rightarrow b} = \tilde{K}_{b \rightarrow a} = 0. \quad (9)$$

Then one can easily compute the maximum $a-b$ -flow, i.e., the maximum flow that can be transmitted from node a to node b respecting the upper bound for the flows given by (8). Several algorithms have been developed for this task, such as the algorithm of Edmonds and Karp and the algorithm of Ford and Fulkerson [36]. The value of the maximum $a-b$ -flow quantifies the redundancy of the grid with respect to the failure of the link (a, b) and will thus be referred to as the *redundant capacity* K_{ab}^{red} in the following. If this value is larger than $F_{ab}^{(0)}$, then a solution of the flow problem defined by equations (6) and (7) exists. Hence a necessary condition for the existence of a stable steady state after the outage of a link (a, b) is given by

$$F_{ab}^{(0)} \leq K_{ab}^{\text{red}}. \quad (10)$$

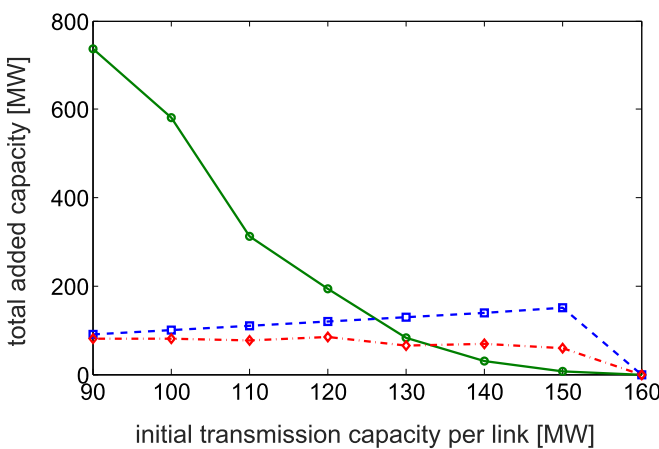


Figure 6. Comparison of strategies as in figure 4, but for a ring topology with one rewired link. We compare the three strategies defined in section 4: A: duplicating the critical line (blue dashed) B: adding a backup line of minimum capacity locally (red dash-dotted) C: adding capacity at bottlenecks nonlocally (solid green).

This condition allows us to understand the main aspects of the flow rerouting problem and to identify bottlenecks in the grid via the *max-flow-min-cut theorem* [36]. Consider a partition (V_1, V_2) of the vertex set V such that $a \in V_1$ and $b \in V_2$ (also called an a - b -cut of the graph). The edges connecting the two parts V_1 and V_2 (called the induced cutset)

$$E(V_1, V_2) = \{\text{edge } (j, \ell) | j \in V_1, \ell \in V_2\} \quad (11)$$

provide a certain amount of capacity for flow rerouting:

$$\tilde{K}_{V_1, V_2} = \sum_{j \in V_1, \ell \in V_2} \tilde{K}_{j \rightarrow \ell}. \quad (12)$$

The max-flow-min-cut theorem now states that the maximum a - b -flow is equal to the minimum capacity over all a - b -cuts such that

$$K_{ab}^{\text{red}} = \min_{V_1, V_2} \tilde{K}_{V_1, V_2} \quad \text{with } a \in V_1, b \in V_2. \quad (13)$$

The max-flow-min-cut theorem now tells us what to do if the necessary condition (10) for $N - 1$ -stability is violated. To increase K_{ab}^{red} above $F_{ab}^{(0)}$ we must add at least the capacity

$$K_{ab}^{\text{add, min}} = F_{ab}^{(0)} - K_{ab}^{\text{red}}. \quad (14)$$

Furthermore, the max-flow-min-cut theorem also tells us *where* to extend the grid. So let $V = V_1 + V_2$ be the partition of the vertex set for which the minimum in equation (13) is attained and $E(V_1, V_2)$ the induced cutset. The transmission lines in $E(V_1, V_2)$ are the bottlenecks for the flow rerouting from a to b —they are fully loaded when the maximum a - b -flow is realized. To increase this maximum flow, we have to extend the transmission capacity between the two vertex sets V_1 and V_2 . One obvious choice is to add another direct connection (a, b) as used for the local strategy A. But we can also add transmission capacity at remote places, in particular by extending any transmission line from the cutset $E(V_1, V_2)$. One efficient strategy to localize a link in $E(V_1, V_2)$ is again provided by the Edmonds–Karp algorithm. This algorithm calculates the maximum a - b -flow by finding shortest paths from a to b and adding flows along these paths. In this sense we propose the following strategy (strategy C in the following) to increase K_{ab}^{red} in a nonlocal way:

- Calculate the shortest path from a to b after the link (a, b) has been removed.
- Localize the bottleneck along the path.
- Increase the capacity of this bottleneck.

This strategy is particularly efficient if there is only one ‘critical’ cutset, i.e., only one cutset $E(V_1, V_2)$ which limits the maximum a - b -flow, while all other links on the rerouting pathways have enough transmission capacity $\tilde{K}_{j, \ell}$ left. Then the extension of a single line in $E(V_1, V_2)$ is sufficient to restore the condition (10). In general there can be several bottlenecks along a rerouting pathway, which limit the maximum flow from a to b . Then we have to iterate the procedure as detailed in the next section.

We emphasize that condition (10) is necessary but not sufficient for the existence of a stable steady state after the outage of a line (a, b) for two reasons. First, the flows in a power grid cannot be chosen arbitrarily but are determined by the phases $(\theta_1, \dots, \theta_N)$ at each oscillator via equation (2). Hence it is possible that a suitable a - b -flow exists, but that we cannot find phases such that $F_{j\ell}^{(0)} + \Delta F_{j\ell} = K_{j\ell} \sin(\theta_j - \theta_\ell)$ for all links (j, ℓ) [37]. Secondly, there may be a transient effect causing a desynchronization. After the loss of a transition line (a, b) there can be a coexistence of a stable fixed point with a limit cycle [38]. Then it is possible that the system converges to the limit cycle and loses synchrony although a stable operation is possible in principle [18].

4. Curing strategies

In this section we describe how to operationalize the local and nonlocal strategies to extend the grid to restore $N - 1$ -security. First we identify critical links by removing single links from the network and recording the time evolution of all rotator phases and their velocities. For stable links the phase differences become constant over time, and the common frequency is the desired grid frequency. For critical links, deviations from the net frequency outside a tolerance interval remain, which would lead to an emergency shutdown of parts of the power grid in real-world power grids (see figure 2 for an example). We then analyze three different strategies to stabilize critical links.

Strategy A: A straightforward local strategy is to build identical backup links for the critical links, i.e., to increase the grid's redundancy locally at the places, where critical failures take place.

Strategy B: As argued in the previous section we typically need less backup capacity to restore $N - 1$ -security, a lower bound being given by expression (14). So, as a variation of strategy A we insert a backup link of minimum capacity. In practice, we increase the transmission capacity of the backup line in steps of 0.1 K until the grid becomes stable with respect to an outage of the critical line (a, b) .

Strategy C: Furthermore, we can also increase the grid's redundancy non-locally by extending bottleneck links along rerouting pathways as discussed in the previous section. If we find a critical link (a, b) , we localize the bottleneck on the shortest rerouting path and increase its capacity. We iterate this procedure if necessary until the link (a, b) becomes stable. If there is no rerouting path, the critical link (a, b) is a bridge. These links are trivially critical, so we exclude these links from our analysis.

Schematically, we use the following algorithm for strategy C: for a given uniformly chosen capacity $K_{j\ell}$ calculate the load distribution in the normal operation of the grid. Sort the links in an arbitrary sequence. Start the loop over all links (a, b) :

- (1) Determine whether link (a, b) of the sequence is critical:
 - (a) Eliminate (a, b) , i.e., set $K_{ab} = 0$ and run the dynamics.
 - (b) If the system approaches a stable state with $\dot{\theta}_i = 0$ for all nodes i , go to the next link in the sequence without any update, otherwise the link is identified as critical.
 - (2) If the link (a, b) is critical, find and strengthen the bottleneck:
 - (a) Calculate the shortest path p from a to b in the residual network and identify the bottleneck, i.e., the link (j, ℓ) for which the residual capacity

$$K_{j\ell} - F_{j\ell}^{(0)} \quad (15)$$
 assumes its minimum along the path p .
 - (b) Increase the capacity at the bottleneck

$$K'_{j\ell} = c K_{j\ell}. \quad (16)$$
- Here we choose $c = 1.1$.
- (c) Determine whether the link is still critical despite the increased capacity. If no, go to the next link.
 - (d) If yes, repeat the procedure, i.e., GOTO step (a).
- (3) Calculate the sum of the increase in capacities along the bottlenecks of all critical links to decide which strategy is superior if all critical links of a whole network should be cured.

A few remarks are in order. The algorithm always increases the capacity along the shortest rerouting path as inspired by the Edmonds–Karp algorithm, which is conceptually simplest. The restriction to the shortest paths seems to be justified in the network with the topology of the Romanian grid, as we have explicitly checked. An

example of flow rerouting for a stable link is shown in figure 3. One clearly sees that the flow changes $|\Delta F_{j\ell}|$ are largest along the shortest alternative paths. We tested the redistribution of flows for other stable links and found similar decay behavior for all tested links in the Romanian grid. In cases where the change in the flow decays only slowly with the distance from the critical link such as discussed in [39], one should include longer paths in more remote areas of the grid, which connect node a with b . The decay behavior in the flow rerouting problem is discussed in detail in [39–42].

Our strategy applies to transmission line overloads, but does not capture voltage instabilities. For models dealing with transmission line overloads, the strategies are generally independent of the specific model system. The strategies A, B and C can be applied for other dynamics. For strategy C the steady state of the dynamics determines the bottlenecks, whereas strategies A and B work in the same way for any dynamics. Other improved or refined models may replace the oscillator dynamics, as long as they satisfy the continuity equation for flows, and losses along the lines are negligible.

5. Performance of curing strategies

5.1. Curing the Romanian power grid

We test the performance of the strategies using a synthetic network, sharing the topology with the Romanian high voltage power transmission grid [35] as illustrated in figure 1 and the distribution of generators and consumers including their actual values for production and consumption. However, we discard all connections to neighboring countries and keep only the internal lines of Romania. The net power injection at the 66 substations is negative with $P \in [-400, 0]$ MW, i.e., these nodes act as consumers (blue circles in figure 1). There are 22 substations with positive power injection and $P \in [24, 1108]$ MW (green diamonds). For simplicity we assume that the transmission capacity of all links is equal, i.e., $K_{j\ell} \equiv K$ for all lines (j, ℓ). Furthermore, we vary the value of K to interpolate between a weakly (K large) and a strongly (K small) loaded grid.

The different strategies for improving network resilience are compared in figure 4. Obviously, the naive addition of backup links by strategy A performs worst. A large amount of capacity (twice the original capacity of all critical links) has to be added to make the grid $N - 1$ -secure. We note that the steps in the curve are due to the fact that the added capacity is directly proportional to the number of critical links, which changes abruptly as a function of the initial capacity. The slight increase between succeeding steps results from the fact that the added line for replacement of the critical link is equipped with the same capacity as the critical link was before its removal.

Remarkably, the performance of the two alternative strategies B and C is very similar. This corresponds to our graph-theoretical analysis of the flow rerouting problem in section 3: if we can attribute a critical link (a, b) to exactly one critical cutset, then it makes no difference if additional capacity is added locally or along one of the bottleneck links in the cutset. In practice differences arise for example due to transient effects. Our numerical results show that the difference in the total added capacity is rather small when adding capacity locally or nonlocally.

The total added capacity can be estimated from the redundant capacity in the sense of providing a lower bound. For one particular critical link (a, b) we must add at least the capacity $K_{ab}^{\text{add}, \min}$ defined in equation (14) to restore $N - 1$ -stability. Assuming that the critical lines are uncorrelated, i.e., that they are not caused by the same bottleneck, we thus obtain the following lower bound for the total added capacity

$$K_{\text{tot}}^{\text{add}, \min} = \sum_{(a,b) \text{ critical}} (F_{ab}^{(0)} - K_{ab}^{\text{red}}) \times \mathcal{I}(F_{ab}^{(0)} > K_{ab}^{\text{red}}), \quad (17)$$

where \mathcal{I} denotes an indicator function which is one if the condition in the argument is true and zero otherwise. Indeed this formula provides a reasonable estimate for the total added capacity in the network under consideration (see figure 4). Obviously, the total numerical value is slightly higher since the graph-theoretical considerations provide only necessary conditions for $N - 1$ -stability. For instance, several bottlenecks may be found along the paths for one critical link so that the added capacity in the algorithm would be larger, or the readjustment factors c in the algorithm have not been chosen optimally small.

5.2. Random graphs

We further compare the different curing strategies for generic random network ensembles. We first consider random networks of the Erdős Renyi type [43], again with 100 nodes (five large generators with $P = 100$ MW, ten small ones with $P = 35$ MW and 85 consumers with $P = -10$ MW placed at random locations in the grid). Results are shown in figure 5 for two different values for the mean degree, connecting any randomly chosen pair of nodes with probability (a) 4/100 or (b) 6/100, respectively. Hence each node is connected with four or six other ones on average. Each link has the same transmission capacity K . For both connection probabilities,

different realizations of the grid need different initial capacities K_{\min} that are minimally required for reaching a stable state. We then compare and average only over grids with similar K_{\min} . Here we consider a minimal transmission capacity of $K_{\min} = 34$ MW for an average of four connections and of $K_{\min} = 46$ MW for six connections. In both cases we take the average over fifty random realizations.

The numerical results confirm our analysis for the Romanian test grid. The performance of strategies B and C is comparable and in any case much better than the naive strategy A. For a mean degree of 6 (figure 5 (b)), the local strategy B performs slightly better. This confirms the view that it is typically of minor importance whether capacity is added locally or nonlocally at the position of the bottlenecks.

5.3. Ultrasparse networks

The effectiveness of the nonlocal strategy C relied on the assumption that we can attribute each critical link to one remote bottleneck in the grid. This assumption can fail in specific network topologies. If there are several bottleneck links along a rerouting pathway, strategy C requires to extend all these bottlenecks whereas only one link has to be added in strategy B. On the contrary, if a single bottleneck causes several other links to be critical, we can stabilize the entire grid by extending just this bottleneck using strategy C. Strategy B would require to add capacity for every critical link separately.

We illustrate these effects for an ultrasparse network. As before we consider a network with 100 nodes and randomly assign five large generators with $P = 100$ MW, ten small ones with $P = 35$ MW and 85 consumers with $P = -10$ MW to the nodes. The topology is a ring with a single rewired link, i.e., a small-world topology in the limit of an almost regular topology [44]. In particular, we start from a simple ring where every node is connected to its nearest neighbors only. Then we randomly delete one heavily loaded link connected to a large generator and reinsert it at a different location so that the ring is broken into a loop and an attached chain. All links have the same transmission capacity K .

Depending on the initial value of the transmission capacity K , strategy B or C may be superior, as demonstrated in figure 6. The single rewired link is always critical. When this critical link fails, power flow has to be rerouted along the entire loop, where several bottlenecks are present for low K . In the nonlocal strategy C we have to extend all these bottleneck separately, which is very costly. Indeed we find that the local strategies A and B outperform strategy C by far in this case.

The situation is reversed when K is larger. The rewired link remains critical but there is only one bottleneck left in the grid which can be effectively extended using strategy C. Indeed we find that the total added capacity is smallest for strategy C for $K \geq 140$ MW.

6. Conclusions and outlook

Single link failures may induce global outages in power grids and other complex supply networks. The design of future grids which ensure $N - 1$ security is generally based on large-scale numerical simulations. In this article we contribute to a better theoretical understanding of network resilience and optimization by comparing local and nonlocal strategies to extend existing grids.

Building local backup lines is a straightforward option to maintain $N - 1$ -security, but elementary graph-theoretic arguments show that the same result can often be achieved by a different, nonlocal strategy. To enable flow rerouting after a link failure, the grid must provide enough redundant capacity along alternative pathways. If this is not possible, we can equally well build a new backup locally or strengthen the alternative pathways nonlocally. Based on these considerations we describe in detail an algorithm to identify and strengthen bottlenecks along short rerouting pathways.

Local and nonlocal strategies are comparable if each critical link can be attributed to one bottleneck. Then it is insignificant whether we add capacity locally or at the bottleneck and we can estimate the necessary grid extensions from the redundant capacity. This scenario was confirmed by numerical simulations for a real-world grid topology as well as for random networks. Strong differences between the strategies were found in an ultrasparse network. If such a grid is heavily loaded, there are typically several bottlenecks along a rerouting path such that the nonlocal strategies perform significantly worse than local strategies. On the contrary, a single bottleneck can cause several links to be critical in the case of weak loads. Then the nonlocal strategy is clearly superior as it cures all critical lines by strengthening a single bottleneck.

We note that the results presented above make no immediate conclusions about real-world power grids due to several simplifications in the model class itself. Yet, given the generic dynamics and conservation laws on flow and supply networks, we are confident that this article may contribute to a better understanding of collective properties of flow and supply networks. It may also provide valuable hints about the operation of real-world power grids, where more detailed studies for more specific systems and settings might reveal specifically tailored counter actions for a power system under consideration. Taken together, our results indicate that non-local

rerouting of flows upon link failure often provides a viable complement to local updates. In power grids, taking into account non-local rerouting along the lines of our strategy C may enhance our options to satisfy the $(N - 1)$ -criterion in a more efficient way.

Acknowledgments

We gratefully acknowledge support from the Federal Ministry of Education and Research (BMBF grant no. 03SF0472A-E), the Deutsche Forschungsgemeinschaft (DFG grant no. ME-1332/19-1 to MR and HM-O), the Helmholtz Association (via the joint initiative ‘Energy System 2050—A Contribution of the Research Field Energy’ and the grant no. VH-NG-1025 to DW) and the Max Planck Society to MT.

References

- [1] Turner A 1999 *Science* **285** 687
- [2] Sims R et al 2011 Integration of renewable energy into present and future energy systems *IPCC Special Report on Renewable Energy Sources and Climate Change Mitigation* ed O Edenhofer et al (Cambridge: Cambridge University Press)
- [3] Pesch H, Allelein H-J and Hake J-F 2014 *Eur. Phys. J. Spec. Top.* **223** 2561
- [4] Heide D, von Bremen L, Greiner M, Hoffmann C, Speckmann M and Bofinger S 2010 *Renew. Energy* **35** 2483
- [5] Rasmussen M G, Andresen G B and Greiner M 2012 *Energy Policy* **51** 642–51
- [6] Milan P, Wächter M and Peinke J 2013 *Phys. Rev. Lett.* **110** 138701
- [7] Rohden M, Sorge A, Timme M and Witthaut D 2012 *Phys. Rev. Lett.* **109** 064101
- [8] Schäfer B, Matthiae M, Timme M and Witthaut D 2015 *New J. Phys.* **17** 015002
- [9] Amin S M and Wollenberg B F 2005 *IEEE Power Energy Mag.* **3** 34
- [10] Fairley P 2004 *IEEE Spectr.* **41** 22–9
- [11] Pourbeik P, Kundur P S and Taylor C 2006 *IEEE Power Energy Mag.* **4** 22–9
- [12] Hines P, Apt J and Talukdar S 2009 *Energy Policy* **37** 5249–59
- [13] Union for the Coordination of Transmission of Electricity 2007 Final report on the system disturbance on 4 November 2006 (<http://entsoe.eu/library/publications/ce/otherreports/Final-Report-20070130.pdf>)
- [14] Brummitt C D, Hines P D, Dobson I, Moore C and D’Souza R M 2013 *Proc. Natl Acad. Sci.* **110** 12159
- [15] Helbing D 2013 *Nature* **497** 7447
- [16] Albert R, Jeong H and Barabási A 2000 *Nature* **406** 378
- [17] Albert R, Albert I and Nakarado G 2004 *Phys. Rev. E* **69** 025103
- [18] Simonsen I, Buzna L, Peters K, Bornholdt S and Helbing D 2008 *Phys. Rev. Lett.* **100** 218701
- [19] Buldyrev S V, Parshani R, Paul G, Stanley H E and Havlin S 2010 *Nature* **464** 1025
- [20] Schneider C M, Moreira A A, Andrade J S, Havlin S and Herrmann H J 2011 *Proc. Natl Acad. Sci.* **108** 3838
- [21] Witthaut D and Timme M 2012 *New J. Phys.* **14** 083036
- [22] Witthaut D and Timme M 2013 *Eur. Phys. J. B* **86** 377
- [23] Kundur P 1994 *Power System Stability and Control* (New York: McGraw-Hill)
- [24] Machowski J, Bialek J and Bumby J 2008 *Power System Dynamics, Stability and Control* (New York: Wiley)
- [25] Schmietendorf K, Peinke J, Friedrich K and Kamps O 2014 *Eur. Phys. J. Spec. Top.* **223** 2577
- [26] Nishikawa T and Motter A E 2015 *New J. Phys.* **17** 015012
- [27] Weckesser T, Johannsson H and Ostergaard J 2013 Impact of model detail of synchronous machines on real-time transient stability assessment 2013 IREP Symp. *Bulk Power System Dynamics and Control-IX Optimization, Security and Control of the Emerging Power Grid (IREP)* p 1
- [28] Auer S, Kleis K, Schultz P, Kurths J and Hellmann F 2016 *Eur. Phys. J. Spec. Top.* **225** 609
- [29] Motter A, Myers S, Anghel M and Nishikawa T 2013 *Nat. Phys.* **9** 191
- [30] Bergen A R and Hill D J 1981 *IEEE Trans. Power Appar. Syst.* **PAS-100** 25–35
- [31] Dörfler F, Chertkov M and Bullo F 2013 *Proc. Natl Acad. Sci.* **110** 2005
- [32] Filatrella G, Nielsen A H and Pedersen N F 2008 *Eur. Phys. J. B* **61** 485
- [33] Rohden M, Sorge A, Witthaut D and Timme M 2014 *Chaos* **24** 013123
- [34] Menck P, Heitzig J, Kurths J and Schellnhuber H J 2014 *Nat. Commun.* **5** 3969
- [35] Hutzcheon N and Bialek J W 2013 Updated and validated power flow model of the main continental European transmission network *Proc. IEEE PowerTech Conf. (New York, 2013)* (IEEE) pp 1–5
- [36] Ahuja R K, Magnati T L and Orlin J B 1993 *Network Flows: Theory, Algorithms, and Applications* (Upper Saddle River, NJ: Prentice-Hall)
- [37] Manik D, Timme M and Witthaut D 2016 arXiv: [1611.09825](https://arxiv.org/abs/1611.09825)
- [38] Manik D, Witthaut D, Schaefer B, Matthiae M, Sorge A, Rohden M, Katifori E and Timme M 2014 *Eur. Phys. J. Spec. Top.* **223** 2527
- [39] Labavic D, Suciu R, Meyer-Ortmanns H and Kettemann S 2014 *Eur. Phys. J. Spec. Top.* **223** 2517
- [40] Kettemann S 2016 *Phys. Rev. E* **94** 062311
- [41] Ronellenfitsch H, Manik D, Brown T, Hörsch J and Witthaut D 2016 arXiv: [1606.07276](https://arxiv.org/abs/1606.07276)
- [42] Jung D and Kettemann S 2016 *Phys. Rev. E* **94** 012307
- [43] Erdős P and Rényi A 1959 *Publ. Math. Debrecen* **6** 290
- [44] Watts D J and Strogatz S H 1998 *Nature* **393** 440